Monthly Notices
of the
ROYAL ASTRONOMICAL SOCIETY

MNRAS **457,** 4262–4271 (2016)
Advance Access publication 2016 January 27

doi:10.1093/mnras/stw209

Observing two dark accelerators around the Galactic Centre with *Fermi* Large Area Telescope

C. Y. Hui,[1⋆] P. K. H. Yeung,[1,2,3] C. W. Ng,[2] L. C. C. Lin,[4] P. H. T. Tam,[5] K. S. Cheng,[2] A. K. H. Kong,[3] D. O. Chernyshov[2,6] and V. A. Dogiel[2,6,7]

[1]*Department of Astronomy and Space Science, Chungnam National University, Daejeon 305-764, Korea*
[2]*Department of Physics, University of Hong Kong, Pokfulam Road, Hong Kong*
[3]*Institute of Astronomy and Department of Physics, National Tsing Hua University, Hsinchu, Taiwan*
[4]*Institute of Astronomy and Astrophysics, Academia Sinica, Taiwan*
[5]*School of Physics and Astronomy, Sun Yat-Sen University, Guangzhou 510275, China*
[6]*I.E.Tamm Theoretical Physics Division of P.N.Lebedev Institute of Physics, Leninskii pr. 53, 119991 Moscow, Russia*
[7]*Moscow Institute of Physics and Technology, 141700 Moscow Region, Dolgoprudnii, Russia*

Accepted 2016 January 21. Received 2016 January 20; in original form 2015 November 4

ABSTRACT

We report the results from a detailed γ-ray investigation in the field of two 'dark accelerators', HESS J1745−303 and HESS J1741−302, with 6.9 yr of data obtained by the *Fermi* Large Area Telescope. For HESS J1745−303, we found that its MeV–GeV emission is mainly originated from the 'Region A' of the TeV feature. Its γ-ray spectrum can be modelled with a single power law with a photon index of $\Gamma \sim 2.5$ from few hundreds MeV–TeV. Moreover, an elongated feature, which extends from 'Region A' towards north-west for $\sim 1^{\circ}.3$, is discovered for the first time. The orientation of this feature is similar to that of a large-scale atomic/molecular gas distribution. For HESS J1741−302, our analysis does not yield any MeV–GeV counterpart for this unidentified TeV source. On the other hand, we have detected a new point source, *Fermi* J1740.1−3013, serendipitously. Its spectrum is apparently curved which resembles that of a γ-ray pulsar. This makes it possibly associated with PSR B1737−20 or PSR J1739−3023.

Key words: pulsars: individual: PSR B1737−30 – pulsars: individual: PSR J1739−3023 – ISM: individual objects: HESS J1745−303 – ISM: individual objects: G359.1−0.5 – ISM: individual objects: 3EG J1744−3011 – ISM: individual objects: HESS J1741−302.

1 INTRODUCTION

Very high energy (VHE; >100 GeV) surveys of our Galaxy with Imaging Atmospheric Cherenkov Telescopes have uncovered a population of γ-ray sources in the TeV regime (e.g. Aharonian et al. 2005, 2006). For Galactic VHE sources, most of them belong to the classes of pulsar wind nebulae (PWNe) or supernova remnants (SNRs). The nature of their VHE emission is primarily identified by their counterparts found at lower energies (e.g. radio, X-ray). Their TeV-to-X-ray flux ratio, $f_{1-10\,\mathrm{TeV}}/f_{2-10\,\mathrm{keV}}$, is typically <2 (cf. Bamba et al. 2007; Matsumoto et al. 2007).

On the other hand, there is a number of VHE sources that no X-ray/radio counterpart has been found which makes the identification of their nature very challenging. In any case, the detection of VHE γ-rays clearly indicates certain kind(s) of acceleration mechanism(s) is/are taking place in these sources, though the details of the processes are unknown. And therefore, these unidentified objects have been coined with the name 'dark accelerators'.

Most of them are extended and concentrated on the Galactic plane which strongly suggests they belong to our Galaxy.[1] Also, they are clustered within $\sim 30^{\circ}$ around the Galactic Centre. The difficulties of finding their counterparts in lower energies can be ascribed to the severe absorption/extinction towards the Galactic Centre. On the other hand, the absorption/extinction is less of an issue in MeV–GeV regime. And therefore, the Large Area Telescope (LAT) onboard *Fermi Gamma-ray Space Telescope* provides the ideal instrument for constraining the nature of these unknown TeV sources at lower energies.

One of the most interesting dark accelerators is HESS J1745−303 (Aharonian et al. 2008; Bamba et al. 2009; Hui et al. 2011). It was first discovered by the HESS Galactic Plane Survey (Aharonian et al. 2006) and was subsequently investigated in details with dedicated follow-up observations (Aharonian et al. 2008). The TeV γ-ray image shows that it consists several spatial components (denoted as Regions A, B and C in Aharonian et al. 2008). Owing to the lack of spectral variability and the insignificant dip among these regions

⋆ E-mail: cyhui@cnu.ac.kr

[1] http://tevcat.uchicago.edu

in the existing data, it was argued that they are originated from a single object (Aharonian et al. 2008).

Searches for the possible X-ray counterpart of HESS J1745−303 have been conveyed with *XMM–Newton* and *Suzaku* (Aharonian et al. 2008; Bamba et al. 2009). None of these observations has resulted in any evidence for non-thermal X-ray continuum emission. This imposes a limiting TeV-to-X-ray flux ratio to be >4 (Bamba et al. 2009) which is larger than the typical value of PWNe and SNRs.

Despite the non-detection of any X-ray continuum, a possible excess of neutral iron Kα line emission is discovered which is originated from the brightest spatial component (i.e. Region A) of HESS J1745−303 (Bamba et al. 2009). It is suggested to be an X-ray reflection nebula, where X-rays from previous Galactic Centre activities were reflected by a molecular cloud in that location (Bamba et al. 2009; see Koyama et al. 1996b for a detailed discussion on X-ray reflection nebulae around the Galactic Centre).

Searching for the molecular/atomic gas towards HESS J1745−303 has been carried out by Hayakawa et al. (2012). They have confirmed that a molecular cloud has a positional agreement with Region A of HESS J1745−303. And it is apparently extended towards north-west. The total mass of interstellar protons including both the molecular and atomic gas to be $\sim 2 \times 10^6\,\mathrm{M}_\odot$ which provides sufficient targets for producing the observed γ-rays through hadronic processes, such as proton–proton collision.

Using the first 29 months of data obtained by *Fermi* LAT, we have detected and examined the GeV emission from HESS J1745−303 (Hui et al. 2011). We found that a simple power law (PL) is sufficient to describe the GeV spectrum with a photon index of ∼2.6. Interestingly, the PL spectrum inferred in the GeV regime can be connected to that of Region A of HESS J1745−303 in 1–10 TeV without any spectral break (cf. fig. 3 in Hui et al. 2011). However, the spatial resolution of the results reported in our previous work did not allow one to discriminate whether the GeV emission is from which spatial component(s) of HESS J1745−303 (cf. fig. 2 in Hui et al. 2011). If such spectrally connected GeV–TeV emission can be confirmed to be originated from Region A, together with the X-ray reflection and molecular cloud on-site, this can shed light on the cosmic ray density and/or the past activities of the Galactic Centre (see discussion in Hui et al. 2011; Dogiel et al. 2015). This provides us with the motivation to revisit this target with the LAT data with a much longer time span and improved calibrations.

Besides HESS J1745−303, we also investigate another dark accelerator HESS J1741−302 in its neighbourhood. The VHE emission of HESS J1741−302 was detected by Tibolla et al. (2008). The TeV centroids of these two sources are separated by ∼1°. Similar to HESS J1745−303, the source apparently comprises two separate spatial components (HESS J1741−302A and HESS J1741−302B). However, its spectral properties in TeV regime were poorly constrained (Tibolla et al. 2008, 2009). Matsumoto et al. (2010) have claimed to found an X-ray counterpart of one component HESS J1741−302A (see fig. 2 in Matsumoto et al. 2010) with *Suzaku*. Its X-ray spectrum can be fitted by a PL with a photon index of $\Gamma \sim 1.1$. And the TeV-to-X-ray flux ratio is found to be ∼6. For the field of another spatial component, HESS J1741−302B, no X-ray counterpart has been found by *Suzaku* except for a serendipitously detected cataclysmic variable candidate (Matsumoto et al. 2010).

Recently, Hare et al. (2016) have performed a high-resolution X-ray search with *Chandra* observations. 19 X-ray sources have been detected in the fields of HESS J1741−302A and HESS J1741−302B. However, the authors concluded that none of these sources is likely to be associated with the VHE emission. The previous X-ray counterpart of HESS J1741−302A claimed by Matsumoto et al. (2010) based on the *Suzaku* data is resolved into a number of faint point sources without any diffuse emission in the high-resolution *Chandra* image. On the other hand, Hare et al. (2016) have suggested that a nearby energetic pulsar PSR B1737−30, which locates at a distance of ∼400 pc and with a characteristic age and spin-down power of $\tau \sim 20$ kyr and $\dot{E} \sim 8 \times 10^{34}$ erg s^{-1}, respectively (Manchester et al. 2005), can possibly contribute relativistic particles and give rise to the observed VHE emission. Searching for the possible GeV counterpart in the third *Fermi* point source catalogue (3FGL; Acero et al. 2015) does not yield any identification (Hare et al. 2016).

In this investigation, we explore the MeV–GeV emission in the field of both HESS J1745−303 and HESS J1741−302 by using a ∼7 yr of *Fermi* LAT data with the latest instrumental responses and background models.

2 OBSERVATION AND DATA REDUCTION

In this analysis, we use the data obtained by LAT between 2008 August 4 and 2015 June 24. The data were reduced and analysed with the aid of *Fermi* Science Tools v10r0p5 package. In view of the complicated environment of the Galactic central region, we adopted the events classified as Pass8 'Clean' class for the analysis so as to better suppress the background. The corresponding instrument response functions (IRFs) 'P8R2_CLEAN_V6' is used in the investigation.

Considering the spectral distortion induced by energy dispersion can be >5 per cent and rises rapidly below 300 MeV, and we are investigating a crowded region around our Galactic Centre, we focused on the photons with energy >650 MeV. We found that including the photons with energies <650 MeV makes the excesses in the regions of HESS J1745−303 and HESS J1741−302 difficult to resolve. Also, the signal-to-noise ratio of γ-ray features concerned in this investigation drops drastically at energies >25 GeV. With the aforementioned considerations, we focused on the analysis in the energy range of 0.65–25 GeV. We further filtered the data by accepting only the good time intervals where the region-of-interest (ROI) was observed at a zenith angle less than 90° so as to reduce the contamination from the albedo of the Earth. In this work, we only consider a source is genuine if it is detected at a signal-to-noise ratio level $\geq 10\sigma$.

3 DATA ANALYSIS

3.1 Spatial analysis

We started with a binned maximum likelihood analysis for a 28° × 28° ROI centred at RA = $17^{\mathrm{h}}41^{\mathrm{m}}52\overset{\mathrm{s}}{.}514$, Dec. = $-29°51'05\overset{''}{.}08$ (J2000), which is approximately the midpoint between HESS J1745−303 and HESS J1741−302. For subtracting the background contribution, we have included the Galactic diffuse background (gll_iem_v06.fits), the isotropic background (iso_P8R2_CLEAN_V6_v06.txt) as well as all the point sources reported by the 3FGL (Acero et al. 2015) within 31° from the ROI centre in the source model. We thawed the spectral parameters of the 3FGL sources within 5° from the ROI centre in the analysis. For the other 3FGL sources, their spectral parameters were fixed at the catalogue values.

Since HESS J1745−303 is catalogued in 3FGL (3FGL J1745.1−3011), it has already included in the source model through the aforementioned procedure. For HESS J1741−302, we added it

in the model by assuming a point source at an nominal position of RA = $17^h41^m00^s$, Dec. = $-30°12'00''$ (J2000)[1] with a simple PL spectrum. With this source model, we performed a preliminary binned likelihood analysis with the aid of the tool GTLIKE. Using this initial result, we examined the significance of γ-ray excess around these two dark accelerators by computing the test-statistic (TS) map with the tool GTTSMAP.

The TS map of the field around HESS J1745−303 is shown in Fig. 1. The γ-ray emission of this source can be detected at a significance of $\sim 22\sigma$ in 0.65–25 GeV. In comparison with the fig. 2 in Hui et al. (2011), we can now resolve the feature much better. It is now clear that most of the MeV–GeV emission of HESS J1745−303 is originated from Region A. Also, an extended feature is detected at $\sim 16\sigma$ in this energy range. It extends towards north-western direction for $\sim 1.^\circ3$. A clump is found at the far end of this feature which locates at RA = $17^h43^m12^s$, Dec. = $-29°21'00''$ (J2000). For estimating its emission properties, we appended it in the source model as a point source with a PL spectrum in the subsequent analysis. It is referred as *Fermi* J1743.2−2921 hereafter.

We have also investigated the hardness of the γ-ray emission from HESS J1745−303 and *Fermi* J1743.2−2921 by repeating the aforementioned analysis in soft band 0.65–4 GeV and hard band 4–25 GeV. HESS J1745−303 is detected at $\sim 19\sigma$ (TS = 355.7) and $\sim 6\sigma$ (TS = 40.1) in soft and hard bands, respectively. On the other hand, *Fermi* J1743.2−2921 is detected at $\sim 13\sigma$ (TS = 178.0) in soft band. But its significance drops below $\sim 3\sigma$ (TS = 7.2) in the hard band.

Examining the TS map of the field around HESS J1741−302 from the aforementioned analysis has revealed two clumps of γ-ray excess. We refer the one located at RA = $17^h40^m06^s$, Dec. = $-30°13'00''$ (J2000) as *Fermi* J1740.1−3013. The position of this source is consistent with that of 1FIG J1739.4−301 which is independently reported by Ajello et al. (2016). Another excess is found at RA = $17^h38^m36^s$, Dec. = $-29°21'00''$ (J2000). We noted that the detection significance of this excess is $<9\sigma$ over ∼6.9 yr, it is below our pre-defined detection threshold. Therefore, we will not further report its detailed properties in this work. But it is kept in the source model throughout the analysis as part of the background estimation. It will be referred as BKG J1738.6−2921 throughout this work.

Based on the aforementioned initial results, we have modified our source model accordingly. In addition to *Fermi* J1743.2−2921, *Fermi* J1740.1−3013 and BKG J1738.6−2921 were also appended to the model by assuming a PL spectrum. On the other hand, the point source component of HESS J1741−302 was removed from the model in view of the non-detection.

With these modifications, we have re-run the likelihood analysis and produced the TS map of the field around *Fermi* J1740.1−3013 which is displayed as Fig. 2. It is detected at a signal-to-noise ratio level of $\sim 10\sigma$. Its peak is apparently offset from HESS J1741−302 by $\sim 0.^\circ4$. Although there is a feature extends eastward and towards HESS J1741−302A, it is only significant at a level of $\sim 6\sigma$. Therefore, we concluded that *Fermi* J1740.1−3013 is a newly detected source which is unlikely to be the counterpart of HESS J1741−302.

We have also analysed *Fermi* J1740.1−3013 in soft and hard bands. While it remains to be detected at $\sim 10\sigma$ (TS = 110.2) in the soft band which is similar to the signal-to-noise ratio level in the full band analysis, its significance drops below 2σ (TS = 2.2) in the hard band.

For further investigating the MeV–GeV morphology of HESS J1745−303 and *Fermi* J1740.1−3013, we produced the background-subtracted γ-ray count maps of these two sources with a pixel size of $0.^\circ1 \times 0.^\circ1$ and computed the brightness profiles along the features. The binning factor of the brightness profiles ($0.^\circ2$) is chosen with a consideration to optimize the signal-to-noise ratio while keeping a reasonable number of data points for model fitting (see below). The results are shown in the left-hand panels of Figs 3 and 4.

To examine the source extent, we have fitted each profile with a Gaussian. For HESS J1745−303, it yields a full width at half-maximum (FWHM) of $2.^\circ3 \pm 0.^\circ3$. We have also examined the brightness profile in an orientation orthogonal to the feature. The best-fitting FWHM is $1.^\circ3 \pm 0.^\circ3$. All the quoted uncertainties of the brightness profile fitting in this work are 1σ.

For comparing the observed brightness profile with that of a point source, we have performed simulation with the tool GTOBSSIM. Taking the point-like PL spectrum of HESS J1745−303 Region A as the input, we have first generated the simulated data set in 0.65–25 GeV for the same integration time and IRFs as the observed data. We then produce the count map and the brightness profile in the same way as aforementioned. We found the FWHM of a point-like source profile is $0.^\circ6$. The simulated profile is overlaid in Fig. 3 for comparison. The observed brightness profile of HESS J1745−303 in the examined orientation differs from that of a point source by $>5\sigma$. On the other hand, the difference between the observed profile in the orthogonal direction is less than 3σ.

We have also examined if this apparently extended feature is a result of the events' uncertainties in the reconstructed incoming direction of photons. We did this by re-running the aforementioned analysis but with only the events belong to the 'PSF3' partition selected. By sacrificing the photon statistics by a factor of ∼4, we produced the background-subtracted count map of the events with the most accurate reconstructed incoming direction.[2] The brightness profile of HESS J1745−303 obtained from the PSF3 data is displayed in the right-hand panel of Fig. 3. The Gaussian fit yields a FWHM of $1.^\circ5 \pm 0.^\circ2$. The profile in the orthogonal orientation has a best-fitting FWHM of $1.^\circ1 \pm 0.^\circ2$. For comparison, the simulated point-like source profile in PSF3 partition has a FWHM of $0.^\circ5$. The difference between the observed profile in PSF3 partition and that expected for a point source is 5σ and 3σ along the feature and its orthogonal orientation, respectively.

For *Fermi* J1740.1−3013, the Gaussian fit to the brightness profiles of full data (left-hand panel of Fig. 4) and the PSF3 data (right-hand panel of Fig. 4) along the east–west orientation yield a FWHM of $1.^\circ9^{+1.0}_{-0.6}$ and $1.^\circ2 \pm 0.^\circ4$, respectively. On the other hand, the FWHM of the observed profile in the orthogonal direction is $1.^\circ7 \pm 0.^\circ4$ (full data) and $1.^\circ6 \pm 0.^\circ4$ (PSF3), respectively. The profile along the east–west orientation is consistent with that in the north–south orientation within the tolerance of the statistical uncertainties.

For comparison, we have simulated the expected profile of a point source by assuming a PL spectrum of *Fermi* J1740.1−3013. The simulated profile has a FWHM of $0.^\circ5$ (full data) and $0.^\circ4$ (PSF3). This only differs from the observed profile by less than 3σ. Therefore, there is no conclusive evidence for the source to be extended.

3.2 Spectral analysis

In the aforementioned binned likelihood analysis, we have assumed a simple PL spectrum for HESS J1745−303, *Fermi* J1743.2−2921

[2] The isotropic model iso_P8R2_CLEAN_V6_PSF3_v06.txt is used for analysing PSF3 data.

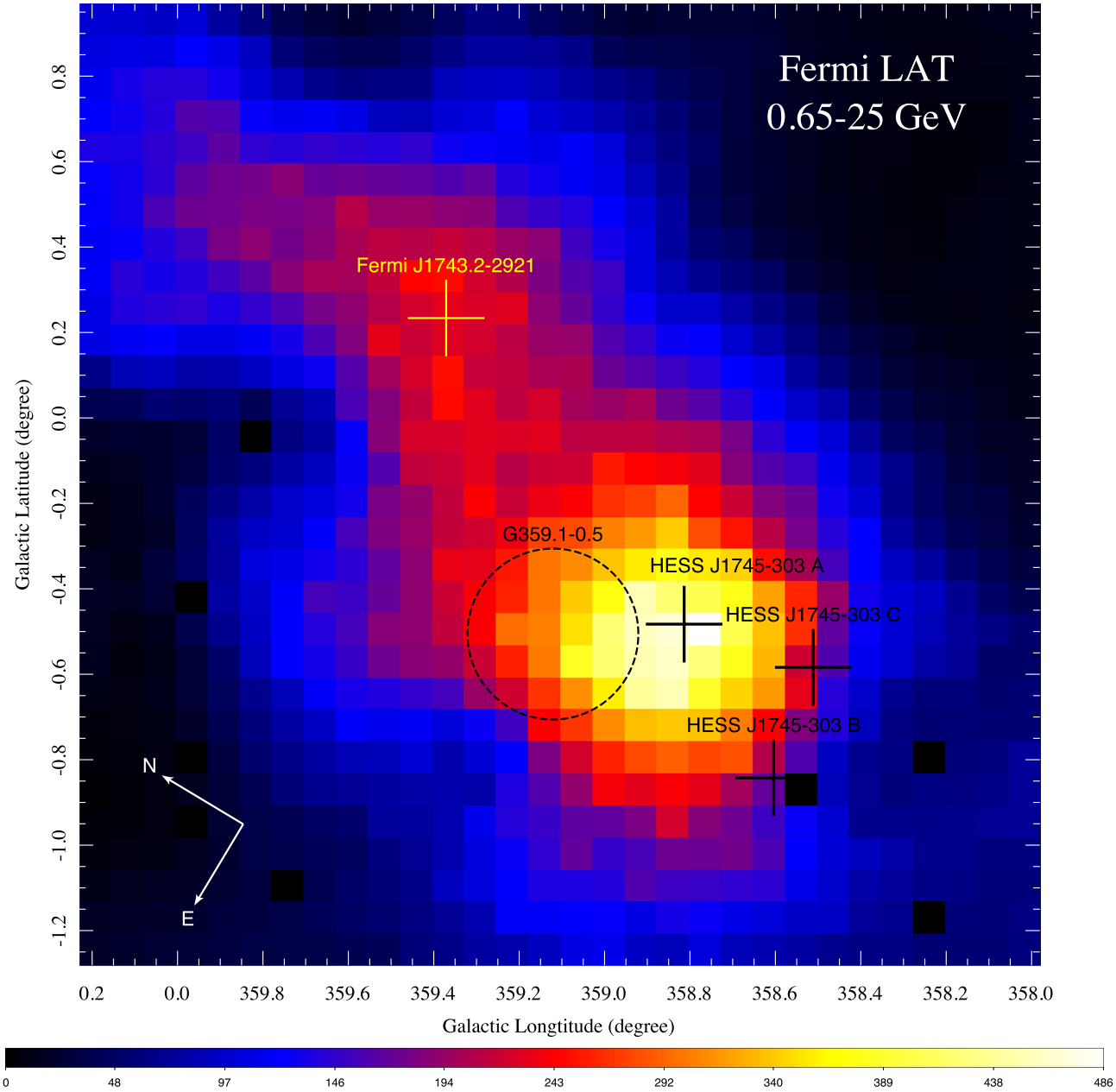

Figure 1. Test-statistic map in 0.65–25 GeV of the field around HESS J1745−303. The nominal emission centres of various TeV components are illustrated by the black crosses (see fig. 1 of Aharonian et al. 2008). The arrows indicate the directions of north and east. We note that there is a feature extends towards north-west. The location of the clump at the end of the feature, *Fermi* J1743.2−2921, is illustrated by the yellow cross. The location of a nearby supernova remnant G359.1−0.5 with a diameter of ∼24 arcmin is illustrated by the dashed circle.

and *Fermi* J1740.1−3013, which yields the photon indices of $\Gamma = 2.68 \pm 0.07$, 2.82 ± 0.11 and 2.60 ± 0.13, respectively. Besides the PL model, we have also examined whether an exponential cut-off power-law model (PLE) or a broken power law (BKPL) can better describe their spectra. The detailed of their spectral properties are summarized in Table 1.

For HESS J1745−303, the additional spectral parameters in BKPL/PLE are not strongly required based on a likelihood ratio test ($<2\sigma$). Therefore, a simple PL model is sufficient to describe its MeV–GeV spectrum. For constructing its spectral energy distribution (SED), we required each bin to attain a signal-to-noise ratio $>4\sigma$ for a robust result. We started with dividing the full energy range into five logarithmically equal spaced energy bins. The binned spectrum is constructed from the independent fitting of each spectral bin. Since the significance of the last bin is below our predefined requirement, the last two bins are combined in the SED. The resultant SED is shown in Fig. 5.

Hui et al. (2011) have suggested that the GeV spectrum of HESS J1745−303 can be connected to the TeV spectrum of Region A (see fig. 3 in Hui et al. 2011). However, ascribing to the difficulty of resolving the GeV emission in this previous study, this spectral connection cannot be confirmed unambiguously. As our spatial analysis shows that the observed MeV–GeV emission is mostly originated from Region A (see Fig. 1), we can re-examine the spectral connection of the spatial component. Fitting the binned spectra obtained by *Fermi* and HESS with a single PL model

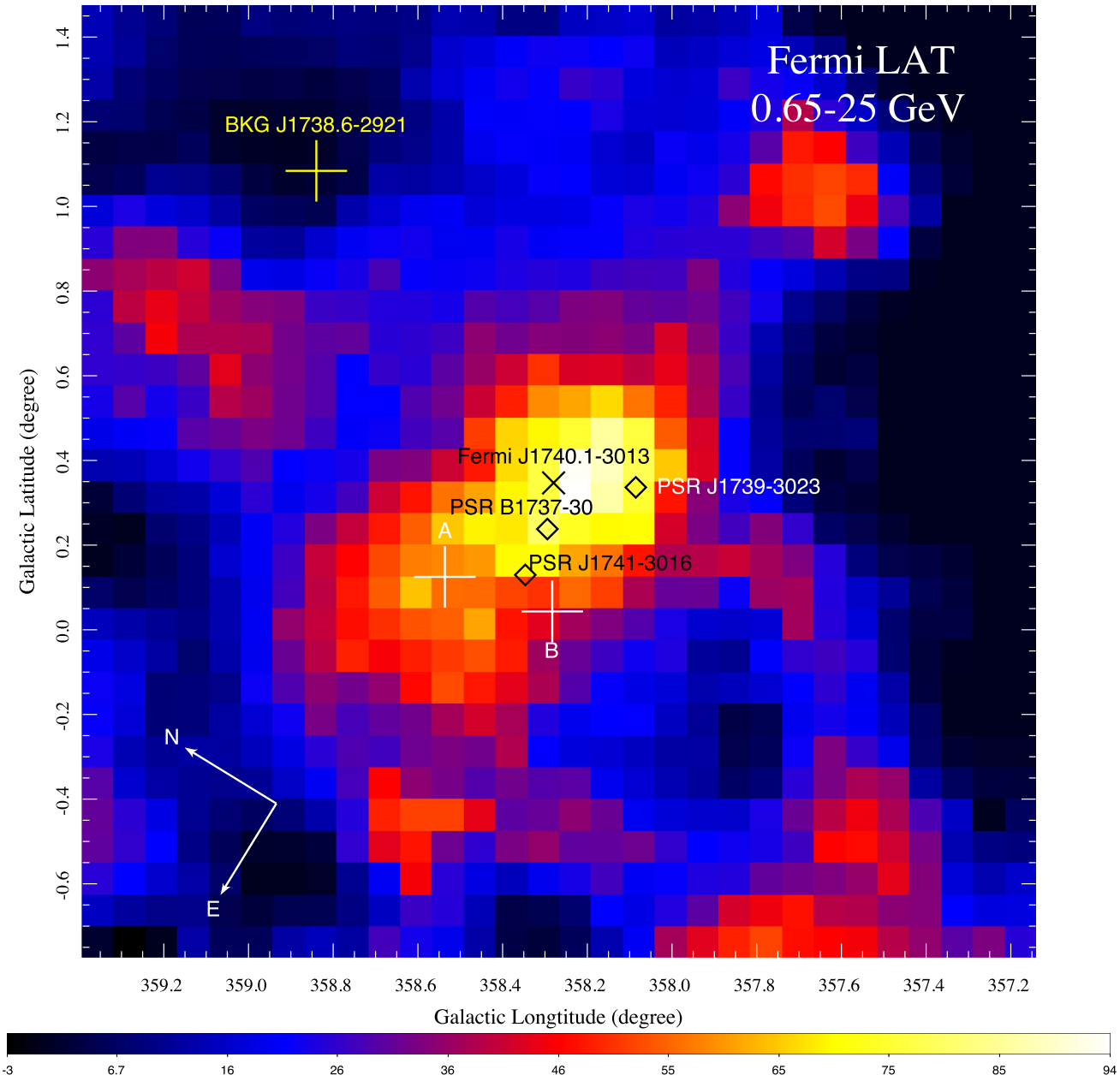

Figure 2. Test-statistic map in 0.65–25 GeV of the field around *Fermi* J1740.1−3013. The nominal emission centres of the TeV components A and B of HESS J1741−302 (cf. Hare et al. 2016) are illustrated by the white crosses. The arrows indicate the directions of north and east. Three pulsars that apparently coincide with the MeV–GeV excess are illustrated by the black diamonds. The location of the point-like background component BKG J1738.6−2921 revealed in this study is illustrated by the yellow cross (see text).

simultaneously yields a photon index of 2.49 ± 0.02 with a goodness-of-fit of $\chi^2 = 9.38$ (7 d.o.f.) which is statistically acceptable.

For the spectrum of *Fermi* J1743.2−2921, namely the clump at the end of the extended feature associated with HESS J1745−303, the simple PL fit results in a photon index which is consistent with that of HESS J1745−303 within the tolerance of 1σ uncertainties. Its SED is shown in Fig. 6. On the other hand, the likelihood ratio test indicates that PLE and BKPL models are preferred over PL by $>4\sigma$. The PLE model yields a photon index of $\Gamma = 1.48 \pm 0.40$ and a cut-off energy of $E_c = 1.90 \pm 0.67$ GeV. For the BKPL model, we found that the spectral break E_b cannot be properly constrained if all parameters are taken as free parameters. Therefore, we have fixed it at $E_b = 2$ GeV for the subsequent analysis. This yields the photon indices $\Gamma_1 = 1.94 \pm 0.24$ and $\Gamma_2 = 3.66 \pm 0.29$ below and beyond E_b, respectively.

For *Fermi* J1740.1−3013, both PLE and BKPL are preferred over simple PL by $>4.5\sigma$. With the break energy fixed at $E_b = 2$ GeV, the BKPL fit yields the photon indices of $\Gamma_1 = 1.51 \pm 0.33$ and $\Gamma_2 = 3.67 \pm 0.42$. For the PLE fit, a photon index of $\Gamma = -0.18 \pm 0.50$ and a cut-off energy of $E_c = 776 \pm 164$ MeV is obtained. We notice that the inferred E_c is very close to the lower bound of our adopted energy range (i.e. 650 MeV). To test the robustness of the PLE fit and check if E_c is stuck in local optima of the parameter space, we repeated the analysis with the lower energy bound shifted to 350 MeV. We found that all the parameters are consistent with

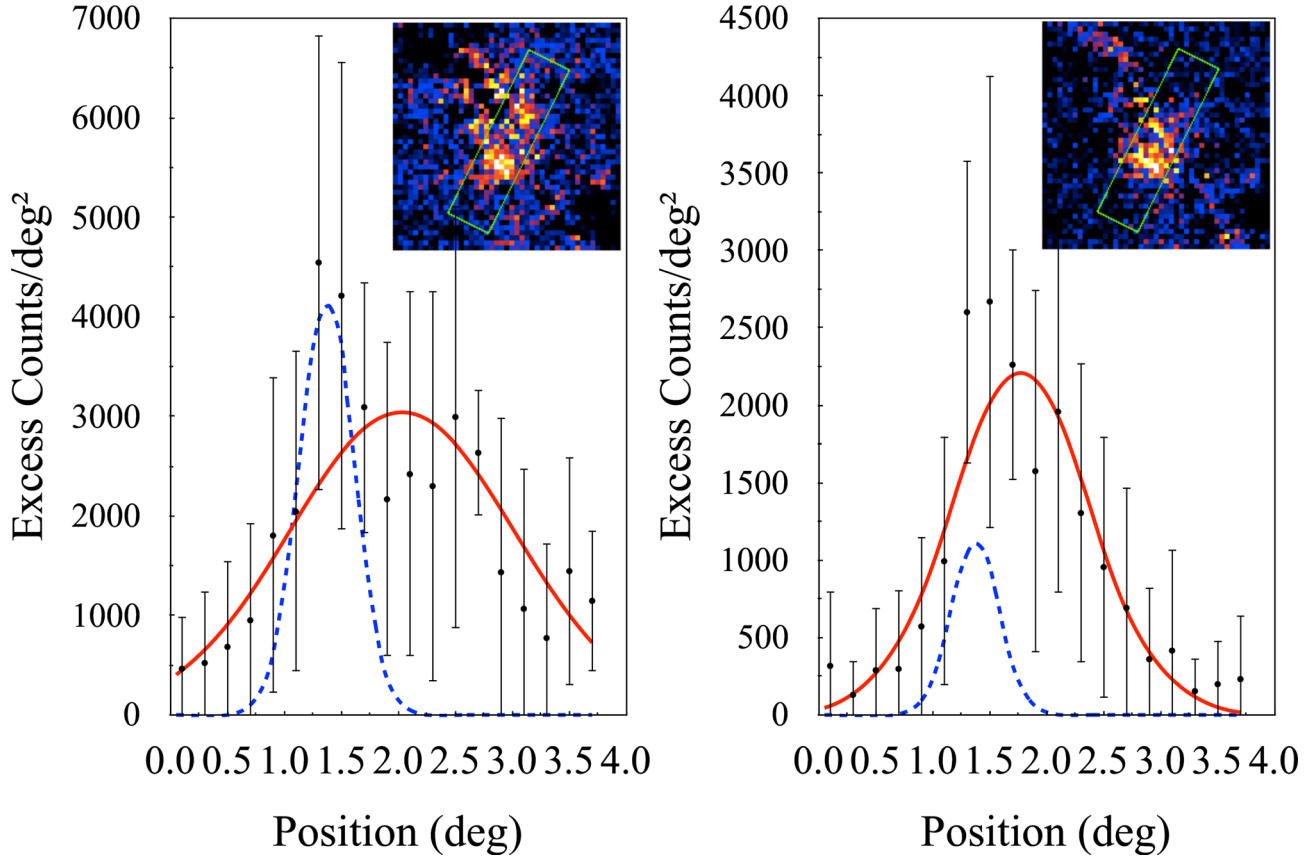

Figure 3. Left-hand panel: the γ-ray brightness profile of HESS J1745−303 computed from the background-subtracted count map in 0.65–25 GeV which is displayed as the inset. The box in the inset illustrates the orientation that the brightness profile is computed. The red curve shows the best-fitting Gaussian model. The blue dashed curve illustrates the expected profile of a point-like source. Right-hand panel: same as left-hand panel but with only the events belong to the PSF3 partition selected.

the previous analysis within the tolerance of statistical uncertainties. The SED of *Fermi* J1740.1−3013 is shown in Fig. 7.

3.3 Searches for long-term variability

In order to examine the long-term variability, we divided the ∼6.9 yr of *Fermi* LAT observation into several segments with a constraint that the source of interest can be detected at a level $>3\sigma$ in each segment. Binned maximum likelihood analysis was performed for individual segment by assuming a simple PL spectral model for each source of interest. Using the γ-ray flux obtained from each time bin, we construct the light curves over a time span of ∼7 yr.

For HESS J1745−303 and *Fermi* J1743.2−2921, the full data set is split into 11 bins each with a size of 230 d. We found that the temporal behaviour of HESS J1745−303 and *Fermi* J1743.2−2921 differs from a uniform distribution at a confidence level of ∼95 and ∼23 per cent, respectively. Hence, there is no evidence of long-term variability for *Fermi* J1743.2−2921. For HESS J1745−303, the variability is marginal. To further investigate its temporal properties, we have repeated the analysis with PSF3 data so as to examine whether the PSF wings of the nearby sources might result in the apparent variability of HESS J1745−303. Adopting the same binning as in the full data set, the confidence level for being a variable drops below 90 per cent in the analysis of PSF3 data. Therefore, there is also no solid evidence for the γ-rays from HESS J1745−303 Region A to be variable.

For *Fermi* J1740.1−3013, since its detection significance is relatively low, we found it is difficult to split the full data set into a reasonable number of time segments and have each to achieve a signal-to-noise ratio level $>3\sigma$ at the same time. Therefore, we are not able to perform any conclusive investigation for its long-term variability in the current study.

4 DISCUSSION AND SUMMARY

We have investigated the γ-ray emission from the fields of HESS J1745−303 and HESS J1741−302 by using ∼7 yr of data obtained by *Fermi* LAT. With the data of improved calibration, we found that the MeV–GeV emission of HESS J1745−303 is mainly originated from the Region A (cf. Fig. 1). The improved resolution allows us to re-examine and confirm the GeV–TeV spectral connection (cf. Fig. 5) as suggested by our previous study (Hui et al. 2011). We note that all the multiwavelength counterparts, including radio, X-ray and GeV, associated with HESS J1745−303 are from the Region A. This leads us to speculate if the Regions B and C as found by Aharonian et al. (2008) are separate sources which are not physically related to HESS J1745−303.

In probing the origin of the γ-ray emission from HESS J1745−303, a nearby supernova remnant (SNR) G359.1−0.5 has been suggested as the contributor of the observed γ-rays (Aharonian et al. 2008). Through the interactions between the shock from the SNR and the molecular cloud, the γ-ray can be produced. By modelling the X-ray emission from G359.1-0.5, Ohnishi et al.

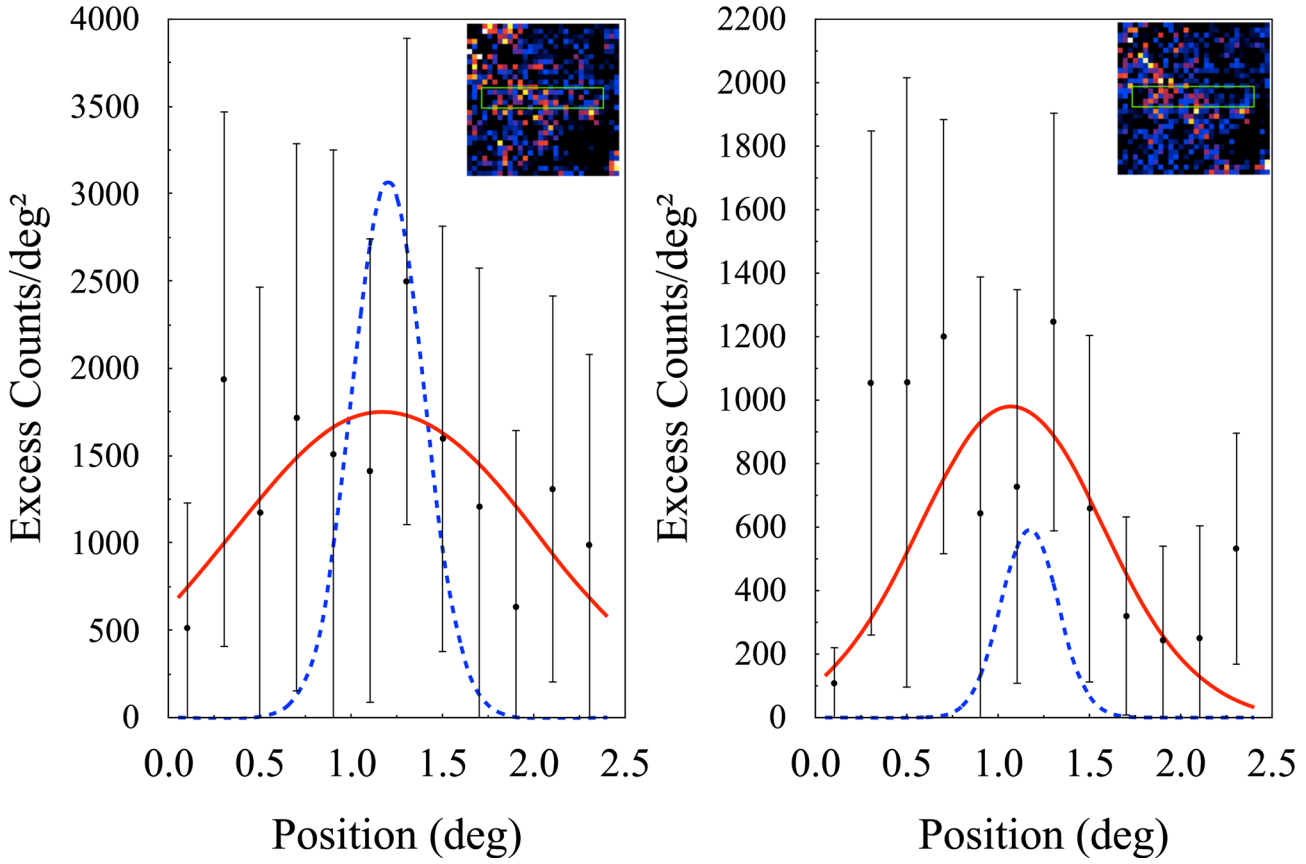

Figure 4. Left-hand panel: the γ-ray brightness profile of *Fermi* J1740.1−3013 computed from the background-subtracted count map in 0.65–25 GeV which is displayed as the inset. The box in the inset illustrates the orientation that the brightness profile is computed. The red curve shows the best-fitting Gaussian model. The blue dashed curve illustrates the expected profile of a point-like source. Right-hand panel: same as left-hand panel but with only the events belong to the PSF3 partition selected.

Table 1. γ-ray spectral properties of HESS J1745−303, *Fermi* J1743.2−2921 and *Fermi* J1740.1−3013 as observed by *Fermi* LAT.

	HESS J1745−303	*Fermi* J1743.2−2921	*Fermi* J1740.1−3013
	PL		
Γ	2.68 ± 0.07	2.82 ± 0.11	2.60 ± 0.13
Photon flux (10^{-9} photons cm^{-2} s^{-1})[a]	14.20 ± 0.86	10.15 ± 0.90	5.89 ± 0.72
TS	398.7	166.3	93.36
	PLE		
Γ	1.95 ± 0.28	1.48 ± 0.40	-0.18 ± 0.50
E_c (MeV)	3619.62 ± 1545.01	1897.6 ± 672.576	775.919 ± 164.014
Photon flux (10^{-9} photons cm^{-2} s^{-1})[a]	13.59 ± 0.85	9.78 ± 0.88	5.50 ± 0.63
TS	402.67	186.78	117.26
	BKPL		
Γ_1	2.09 ± 0.15	1.94 ± 0.24	1.51 ± 0.33
Γ_2	3.18 ± 0.18	3.66 ± 0.29	3.67 ± 0.42
E_b (MeV)	2000	2000	2000
Photon flux (10^{-9} photons cm^{-2} s^{-1})[a]	13.39 ± 0.87	9.69 ± 0.88	5.63 ± 0.69
TS	402.26	184.05	113.66

[a]The energy range of the quoted photon flux in 0.65–25 GeV.

(2011) found that the plasma of this mixed-morphology (MM) SNR is overionized. This property has also been observed in other γ-ray emitting MM SNRs such as IC 443 (Yamaguchi et al. 2009) and W49B (Miceli et al. 2010). The γ-ray luminosities of MM SNRs in 0.1–100 GeV lie in the range of $\sim 10^{35}$–10^{36} erg s^{-1} (see Bamba et al. 2015). At a distance of 8.5 kpc, the γ-ray luminosity of HESS J1745−303 in this band is 1.1×10^{36} erg s^{-1} which is marginally consistent with the range of other MM SNRs.

The γ-ray spectra of many GeV-detected SNRs are soft and show a break at energies of a few GeV (Acero et al. 2015), which suggest the escape of high-energy particles from the acceleration sites. However, there is no evidence for any spectral break to be found in the case of HESS J1745−303. The difference in the GeV spectral shape has put the association between HESS J1745−303 and G359.1−0.5 in question.

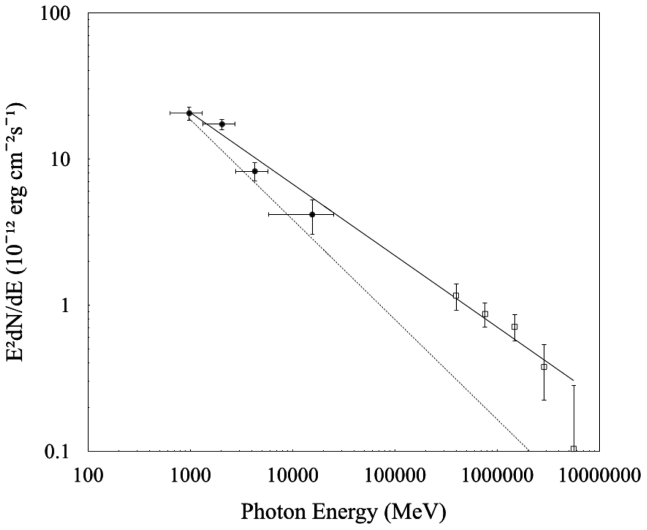

Figure 5. SED of the Region A of HESS J1745−303 as observed by *Fermi* LAT (solid circles) and HESS (open squares). The dashed line illustrates the PL model ($\Gamma = 2.68$) resulted from the likelihood analysis of the *Fermi* LAT data. The solid line represents the best-fitting PL model ($\Gamma = 2.49$) resulted from the simultaneously analysis of both *Fermi* and HESS data.

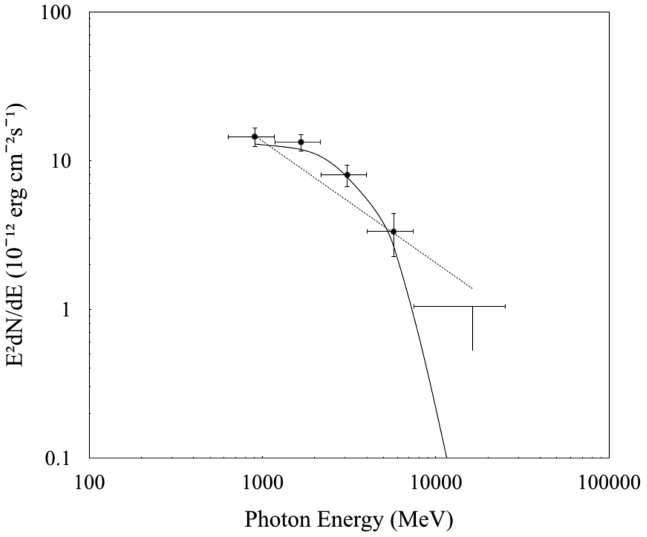

Figure 6. SED of *Fermi* J1743.2−2921. The solid line and the dotted line illustrate the best-fitting PLE and PL models, respectively. The last bin shows the 2σ upper limit.

Since the Region A of HESS J1745−303 is associated with a molecular cloud, the γ-ray emission at this location can be generated by cosmic rays (CRs) penetrating into the clouds from outside. CRs could be provided by supernova remnants from the Galactic disc. These CRs are distributed more or less uniformly throughout the Galaxy with some excess in the Galactic Centre (about a factor of 2 in comparison with the local CR density near the Earth).

Assuming the observed γ-rays are originated from the CRs, we estimate the CR density inside the Region A of HESS J1745−303. This can be estimated from the γ-ray emissivity per hydrogen atom in the cloud. Hayakawa et al. (2012) have estimated the mass of the cloud in this region as $\sim 2 \times 10^6\,M_\odot$. Together with observed γ-ray flux, this implies an emissivity of $\sim 4.2 \times 10^{-6}$ photons s^{-1} H $atom^{-1}$.

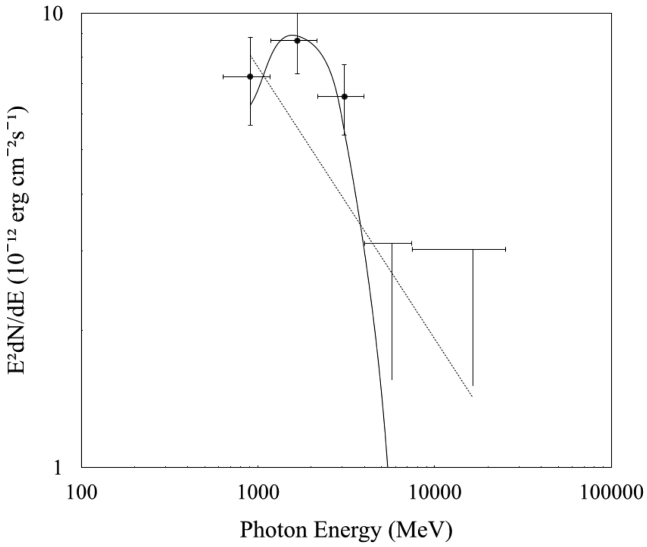

Figure 7. SED of *Fermi* J1740.1−3013. The solid line and the dotted line illustrate the best-fitting PLE and PL models, respectively. The last two bins show the 2σ upper limit.

It is interesting to compare this emissivity with that of the cloud Sgr B2 which is at a distance of ∼100 pc from the Galactic Centre. Its γ-ray spectrum in MeV–GeV regime can be described by PL with $\Gamma \sim 2.5$ (Yang, Jones & Aharonian 2015), which is comparable with that of HESS J1745−303. However, different from the case of HESS J1745−303, it cannot be connected to its TeV spectrum without a break (see fig. 3 in Yang et al. 2015).

The total mass of Sgr B2 possibly ranges from 6 to 15 million solar masses (see Aharonian et al. 2006). According to Yang et al. (2015), the emissivity there is about twice higher than the local value near the Earth. This is in a good agreement with predictions of GALPROP model (e.g. Ackermann et al. 2011) which describes the average distribution of CRs in the Galaxy emitted by SNRs. In Table 2, we compare the emissivities of Sgr B2 and HESS J1745−303 Region A. Their comparable emissivities suggest the CRs inside these clouds have common origin Their γ-ray fluxes are produced by CRs with almost the same background density in the Galactic Centre.

Apart from the bright feature found at the Region A of HESS J1745−303, we have also discovered an elongated γ-ray feature that extends towards north-western direction for $\sim 1^\circ\!.3$ with a clump *Fermi* J1743.2−2921 locates at the end of this feature (see Fig. 1). The photon indices of HESS J1745−303 Region A and *Fermi* J1743.2−2921 inferred from the simple PL fits are consistent within the tolerance of statistical uncertainties. A more detailed investigation of their SEDs suggests the γ-ray spectrum of *Fermi* J1743.2−2921 is likely to be more curved. This may indicate the possible spectral steepening along the extended feature.

Since the newly discovered extended feature is apparently connected to Region A, it is not unreasonable to speculate that the whole feature has a common origin. To test this hypothesis, we encourage an extensive mapping of 6.4 keV line across the whole feature and investigate if the line intensity has any spatial variation. Apart from bombardment by the subrelativistic CRs, the 6.4 keV line can also be generated from a front of hard X-ray photons which were emitted by Sgr A* whose luminosity was much higher in the past than it is at present (Koyama et al. 1996a; Ryu et al. 2013).

Table 2. Comparison of the properties of HESS J1745−303 (Region A) and Sgr B2.

Cloud	Flux >1 GeV 10^{-8} photons s^{-1} cm^{-2}	Mass 10^6 M$_\odot$	Emissivity 10^{-26} photons s^{-1} H atom^{-1}	Reference
Sgr B2	3.5	6–15	1.4–3.5	Yang et al. (2015)
HESS J1745−303	1.4	2	4.2	This work

This can result in a time-varying line flux that has been observed in Sgr B2 (Nobukawa et al. 2014). Therefore, it is also interesting to examine if there is any temporal variability of line flux in Region A by comparing with the results of Bamba et al. (2009).

Another crucial information for probing the origin of the extended feature is the gas distribution in the γ-ray emission region as this can provide targets for producing the observed γ-rays through hadronic processes. We note that the orientation of the extended γ-ray feature detected by *Fermi* is similar to the intensity distribution of ^{12}CO and H I as found by Hayakawa et al. (2012) which has one end at the Region A and extends to north-west (see fig. 2 in Hayakawa et al. 2012). This might indicate the association between the molecular/atomic gas distribution and the γ-ray feature. However, the field investigated by Hayakawa et al. (2012) is less than $1^\circ \times 1^\circ$ which is not wide enough to cover the whole γ-ray feature. Follow-up radio spectral imaging that covers the whole field in Fig. 1 is encouraged for further investigation.

In searching for the MeV–GeV emission from HESS J1741−302, we have discovered *Fermi* J1740.1−3013 which is offset from the TeV emission region by $\sim 0.^\circ 4$ (cf. Fig. 2) which makes it unlikely to be associated with HESS J1741−302. On the other hand, three pulsars are found to be coincide with *Fermi* J1740.1−3013 (see Fig. 2). The apparently curved spectrum of *Fermi* J1740.1−3013 also resembles that of a γ-ray pulsar, though the spectral parameters of the PLE fit cannot be tightly constrained with the current data. In the followings, we discuss the possibilities of these pulsars as a counterpart *Fermi* J1740.1−3013.

PSR J1741−3016 has a spin-down power of $\dot{E} \sim 5 \times 10^{31}$ erg s^{-1} and is located at a distance of $d \sim 5$ kpc. Assuming it is the counterpart of *Fermi* J1740.1−3013, the γ-ray luminosity is $L_\gamma \sim 4.7 \times 10^{34} f_\Omega$ erg s^{-1} at energies >100 MeV, where f_Ω is the solid angle of the beam divided by 4π. Since L_γ exceeds $\dot{E}$ by several orders of magnitude, it is safe to exclude PSR J1741−3016 as the counterpart of *Fermi* J1740.1−3013.

Assuming PSR J1739−3023 is related to *Fermi* J1740.1−3013, with $\dot{E} \sim 3 \times 10^{35}$ erg s^{-1} and $d \sim 3.4$ kpc of the pulsar, a γ-ray conversion efficiency $L_\gamma/\dot{E} \sim 0.07 f_\Omega$ is implied. This is found to be typical for a γ-ray pulsar (cf. Abdo et al. 2013) which makes PSR J1739−3023 as a possible counterpart of this newly detected γ-ray source.

Lastly, we consider the possible association with the nearby pulsar PSR B1737−30 which has $\dot{E} \sim 8 \times 10^{34}$ erg s^{-1} and $d \sim 400$ pc. This implies a conversion efficiency of $L_\gamma/\dot{E} \sim 0.004 f_\Omega$. Therefore, from an energetic point of view, PSR B1737−30 is also a possible counterpart of *Fermi* J1740.1−3013.

To further investigate the physical origin of *Fermi* J1740.1−3013, high-resolution X-ray imaging of its γ-ray emission region is encouraged to look for the X-ray counterparts. This can enable one to compare their X-ray positions with the radio timing position of the aforementioned pulsars. Since the X-ray position can possibly be constrained to subarcsecond accuracy, this can certainly facilitate the pulsation search in γ-ray which can provide the most crucial information for nailing down the nature of this γ-ray source.

ACKNOWLEDGEMENTS

CYH is supported by the National Research Foundation of Korea through grant 2014R1A1A2058590. PHTT is supported by the One Hundred Talents Program of the Sun Yat-Sen University. KSC is supported by a 2014 GRF grant of Hong Kong Government under HKU 17300814P. AKHK is supported by the Ministry of Science and Technology of Taiwan through grant 103-2628-M-007-003-MY3. DOC and VAD acknowledge a partial support from the RFFI grants 15-52-52004, 15-02-02358. CYH, PHTT, KSC, AKHK, DOC and VAD acknowledge support from the International Space Science Institute-Beijing to the International Team 'New Approach to Active Processes in Central Regions of Galaxies'. The author would also like to thank Dr Rui-zhi Yang for the discussion of Sgr B2.

REFERENCES

Abdo A. A. et al., 2013, ApJS, 208, 17
Acero F. et al., 2015, ApJS, 218, 23
Ackermann M. et al., 2011, ApJ, 726, 81
Aharonian F. et al., 2005, Science, 307, 1938
Aharonian F. et al., 2006, Nature, 439, 695
Aharonian F. et al., 2008, A&A, 483, 509
Ajello M. et al., 2016, ApJ, preprint (arXiv:1511.02938)
Bamba A. et al., 2007, PASJ, 59, 209
Bamba A., Yamazaki R., Kohri K., Matsumoto H., Wagner S., Pühlhofer G., Kosack K., 2009, ApJ, 691, 1854
Bamba A., Sawada M., Nakano Y., Terada Y., Hewitt J., Petre R., Angelini L., 2015, PASJ, preprint (arXiv:1509.00214)
Dogiel V. A. et al., 2015, ApJ, 809, 48
Hare J., Rangelov B., Sonbas E., Kargaltsev O., 2016, ApJ, 816, 52
Hayakawa T., Torii K., Enokiya R., Amano T., Fukui Y., 2012, PASJ, 64, 8
Hui C. Y., Wu E. M. H., Wu J. H. K., Huang R. H. H., Cheng K. S., Tam P. H. T., Kong A. K. H., 2011, ApJ, 735, 115
Koyama K., Hamaguchi K., Ueno S., Kobayashi N., Feigelson E. D., 1996a, PASJ, 48, L87
Koyama K., Maeda Y., Sonobe T., Takeshima T., Tanaka Y., Yamauchi S., 1996b, PASJ, 48, 249
Manchester R. N., Hobbs G. B., Teoh A., Hobbs M., 2005, AJ, 129, 1993
Matsumoto H. et al., 2007, PASJ, 59, 199
Matsumoto H., Uchiyama H., Tsuru T. G., Koyama K., Tibolla O., 2010, in Makishima K., ed., The Energetic Cosmos: From Suzaku to ASTRO-H. JAXA Special Publication JAXA-SP-09-008E. p. 154
Miceli M., Bocchino F., Decourchelle A., Ballet J., Reale F., 2010, A&A, 514, L2
Nobukawa M., Nakashima S., Nobukawa K. K., Koyama K., 2014, in Ishida M., Petre R., Mitsuda K., eds, Suzaku-MAXI 2014: Expanding the Frontiers of the X-ray Universe. p. 54
Ohnishi T., Koyama K., Tsuru T. G., Masai K., Yamaguchi H., Ozawa M., 2011, PASJ, 63, 527

Ryu S. G., Nobukawa M., Nakashima S., Tsuru T. G., Koyama K., Uchiyama H., 2013, PASJ, 65, 33
Tibolla O., Komin N., Kosack K., Naumann-Godo M., 2008, in Aharonian F. A., Hofmann W., Rieger F., eds, AIP Conf. Proc. Vol. 1085, High Energy Gamma-Ray Astronomy: Proceedings of the 4th International Meeting on High Energy Gamma-Ray Astronomy. Am. Inst. Phys., New York, p. 249
Tibolla O., Komin N., Kosack K., Naumann-Godo M., 2009, in Bastieri D., Rando R., eds, AIP Conf. Proc. Vol. 1112, Science with the New Generation of High Energy Gamma-Ray Experiments: Proceedings of the 6th Edition: Bridging the Gap Between GeV and TeV. Am. Inst. Phys., New York, p. 233
Yamaguchi H., Ozawa M., Koyama K., Masai K., Hiraga J. S., Ozaki M., Yonetoku D., 2009, ApJ, 705, L6
Yang R.-z., Jones D. I., Aharonian F., 2015, A&A, 580, A90

This paper has been typeset from a TEX/LATEX file prepared by the author.